COMPARATIVE ANALYSIS OF THERMAL ENVIRONMENTS IN NEW YORK CITY AND KUWAIT CITY

Andy Y. Kwarteng[a] and Christopher Small[b]

[a]Remote Sensing and GIS Center; Sultan Qaboos University; Box 33, Al-Khod PC 123, Oman- kwarteng@squ.edu.om
[b]Lamont Doherty Earth Observatory; Columbia University; Palisades, NY 10964, USA- cs184@columbia.edu

KEY WORDS: Surface temperature, New York City, Kuwait City, Urban vegetation, Landsat ETM+, Urban heat island

ABSTRACT:

Satellite-derived thermal information over urban areas offers and attractive and inexpensive method which have been utilized in diverse studies including land cover classification, energy flux interactions, and as input for models of urban surface atmosphere exchange. In this study, we utilize Landsat ETM+ imagery to analyze the dependence of energy fluxes on the urban surface properties in York City and Kuwait City, located in temperate and arid environments, respectively. Thermal imagery is used in conjunction with multispectral imagery to interpret the distribution of surface temperatures in the context of vegetation endmember abundances estimated by spectral mixture analysis. In general, the surface temperatures observed for the surrounding desert areas in Kuwait City are higher than the built-up areas. However, in New York City the suburban areas with more vegetation have relatively lower temperatures than the residential and commercial areas. Even though Kuwait City has lower vegetation fractions, the cooling effect is apparent and is clearly defined in the residential areas. Scatterplots of surface temperature and vegetation fractions define the physical limits imposed by the vegetation cover, soil water content, and different combinations of surface materials in each city. More land cover categories are identified in the New York City than the Kuwait City imagery primarily due to the morphology and location of the two cities.

1. INTRODUCTION

As the world's population continues to grow, rapid urbanization becomes inevitable. Nearly half of the world's human population is now believed to live in urban areas, and for the first time in human history, the figure will surpass 50% by 2007 (United Nations, 2001; UNPF, 2004). Urban sprawl and associated large-scale alteration of the natural landscape will therefore continue to escalate and have a profound effect on environmental conditions and processes. In addition to challenges presented in the area of land use planning, housing, pollution and development, urbanization has received much of attention worldwide due to implications for changes in microclimate, regional scale climates, and impact of potential sea level rises.

As urban areas expand, their surrounding landscapes are dramatically transformed. In tropical and temperate regions, urbanization entails deforestation and loss of agricultural lands. However, in arid and desert areas, such as observed in the Arabian Peninsula, urbanization results in the replacement of barren land with buildings, impervious surface, ornamental trees, and grass. Consequently, urbanization in forest and temperate regions translates to reduction in evapotranspiration, whereas the opposite is true in arid regions. A major objective of city planners is to ensure a healthy and pleasant environment for inhabitants and avoid any harmful repercussion from any large-scale changes. Any effective mitigation techniques should be based on effective long-term monitoring because of the constant changes of urban morphology and environmental conditions.

Near-surface temperature is of critical importance for the study of biosphere processes, terrestrial hydrology, and several Earth science processes, including urban climate (Norman et al., 1995; Czajkowski et al., 2004). It is well known that surface radiant temperature is highly sensitive to vegetation as well as surface soil moisture content (Carlson et al., 1995). Consequently, the availability of reliable surface temperature data over large spatial and temporal scales is crucial for several studies of the urban environment. *In situ* measurements of surface temperature are not generally feasible because of limited sampling density. Thermal infrared information from satellites, which can be converted to brightness temperature through Planck's law, offers an attractive and inexpensive method to measure surface temperature. Such data have been used for diverse studies, including land cover classification, energy flux interactions, and as input for models of urban surface atmosphere exchange. However, the use of thermal observations have been limited to some extent due to the spatial resolutions provided by satellites, and the difficulty in obtaining emissivity values for the various surface materials as well as the incorporation of other variables that affect thermal radiance and energy partitioning at the surface in thermal models. Nevertheless, several useful studies on temperature and urban areas have been conducted (Oke, 1987; Voogt and Oke, 2003).

The most successful applications of remote sensing to the urban environment generally involve measurement of physical quantities related to environmental conditions such as surface temperature and vegetation abundance. The two variables can be combined to provide constraints on the combined effects of spatial variations in albedo, thermal emissivity and evapotranspiration. These spatial variations are a primary determinant of the environmental conditions that influence human comfort levels. The objective of this study is to illustrate some differences in remotely sensed environmental conditions for two cities located in temperate and arid urban areas, respectively. We utilize Landsat ETM+ imagery to analyze the dependence of energy fluxes on the urban surface properties in York City and Kuwait City. Kuwait City is characterized by a desert environment with scanty rainfall, and a dry, hot climate; whereas New York City is located in a temperate climate modulated by the thermal inertia of the Atlantic Ocean. Thermal imagery is used in conjunction with multispectral imagery to interpret the distribution of surface temperatures in the context of vegetation endmember abundances estimated by spectral mixture analysis.

1.1 Urban Physical Environment and Urban Heat Island

The spatial agglomeration of built surface in most cities has different physical characteristics from most naturally occurring environments. In general, the physical environment of a large city is profoundly different from the physical environment of small settlements in rural settings. These physical characteristics influence environmental conditions by changing the flux of mass and energy through the environment. Most of the inhabited areas on Earth are characterized by soil and vegetation but most built environments are dominated by impervious surface and have relatively small amounts of vegetation. Soil retains moisture and allows for continuous evaporation to the atmosphere while impervious surface increase runoff and significantly reduce evaporative moisture flux in the urban environment.

The composition of urban morphologies and their environs results in the phenomenon commonly referred to as urban heat island, which results from the inadvertent urban climate modification from anthropogenic activities (Oke, 1987). Urban materials such as construction material, roofs, asphalt, concrete and roads absorb more heat from the sun. The subsequent release of the energy causes urban areas to be warmer compared to the surrounding non-urban areas giving rise to the urban heat effect (Oke, 1987; Gallo et al., 1995; Lo et al., 1997; Owen et al., 1998; Nichol, 2003; Voogt and Oke, 2003). Urban heat island has been observed and documented for more than one and half centuries (Howard, 1833; Oke, 1987). Depending on the location, the urban heat island effect can be exacerbated by the absence or removal of vegetation, which provides shade and evapotranspiration to cool the air on warm days.

The dynamics of the heat island effect are a function of the time, meteorological conditions, local and urban characteristics, and consequently, could be unique for particular urban areas. In general, parks, lakes and open areas, appear relatively cooler compared to commercial, industrial or dense buildings (Roth et al., 1989). The urban heat intensity, $\Delta T(u-r)$, is the difference between the urban maximum temperature (u) and the non-urban low temperature (r), and is controlled by the unique characteristics of particular urban and suburban areas. For example, in cities with tall buildings, the three-dimensional structures alter the airflow that could reduce heat loss resulting in higher temperatures (Oke, 1987; Nichol, 1996, 1998).

1.2 Importance of Urban Vegetation

The abundance and spatial distribution of vegetation has a strong influence on the urban and suburban environmental conditions. Vegetation influences energy fluxes by selective reflection and absorption of solar radiation. Vegetation has a significant cooling effect because it absorbs much of the incoming solar radiation and dissipates the energy by transpiring water rather than converting the energy to heat and reradiating it as built surfaces do (e.g., Goward et al., 1985; Gallo et al., 1993; Price, 1990; Carlson et al., 1994; Gillies et al., 1997; Owen et al., 1998). This result in different fluxes of moisture and solar radiation, influences comfort levels, and ultimately result in energy savings from cooling. In addition to providing shade and wind shelterbelts, urban trees can lower the ambient temperature around a building or in a park, improve the air quality as well as reduce the formation of urban smog (Akbari, 2002). In cold climates, trees shield buildings from cold winter wind and thereby save energy on heating energy. In warm weather, well-planned landscaping of trees and shrubs can significantly reduce the daily air-conditioning electricity consumption by as much as 50% (Parker, 1981). Well-maintained urban vegetation in the form of trees, grasses, and flowers is visually pleasing, particularly in arid environments where native vegetation is limited by harsh environmental conditions.

1.3 Study Areas

Kuwait City and most parts of the Arabian Shield are characterized by a desert environment with scanty rainfall, and a dry, hot climate. Spring (January to March) temperatures in Kuwait are generally low and quite pleasant compared to the summers, especially July with a mean temperature of 37.4°C and a maximum mean temperature of 45°C. The March average temperature for Kuwait City for the last 50 years is 19.3°C, with a maximum mean temperature of 25.6°C and a mean minimum temperature of 13.2°C. Beyond the limits of Kuwait City, the suburban area consists of flat undulating desert with more than 50% eolian sand surface deposits. During the spring rain season the area supports the growth of ephemeral vegetation. However, desert areas are heavily overgrazed by camels, sheep, and goats, leaving the soil nearly bare most of the time.

The State of Kuwait had embarked on several urban development and facilities management projects to improve the quality of life in Kuwait City since the rapid population growth in the 1970s. In 2004, the population of Kuwait was approximately 2.7 million compared to two million in 1997, 467 thousand in 1965, and 206 thousand in 1957, respectively. Local landscaping, greening and beautification projects were initiated in the 1960s. The latest phase is a comprehensive greenery development plan setup in 1996 as a source of national pride and to enhance economic productivity. The project aims to significantly increase greening in Kuwait City over a 20-year planning period.

New York, in contrast, is characterized by a temperate climate modulated by the thermal inertia of the Atlantic Ocean. Annual temperatures generally range from –20° to 40°C with seasons dictated by temperature rather than precipitation cycles. Contrary to popular belief, the New York metro area is characterized by abundant urban and suburban vegetation in the form of mature deciduous street trees and numerous parks and public green spaces. The population of New York City has not changed dramatically over the last couple of years. However, in the study area, built-up areas have expanded rapidly into the suburban agricultural areas.

2. SURFACE TEMPERATURE AND VEGETATION ANALYSES

Brightness temperatures (also referred to as blackbody temperatures) can be derived from satellites' thermal infrared measurements through Planck's law (Flynn et al., 2001; Dash et al., 2002). The digital numbers of Landsat TM and ETM+ thermal infrared band 6 (10.4-12.5 μm) are converted into radiance using the equation:

$$L_\lambda = gain * DN + offset \quad (1)$$

where L_λ is at sensor radiance, *DN* is the digital number of a pixel, *gain* is slope of the radiance *DN* conversion function in $Wm^{-2}sr^{-1}$ μm^{-1}, offset is the rescaled bias which is the intersection of the radiance DN conversion function in $Wm^{-2}sr^{-1}$ μm^{-1} (Landsat Project Science Office, 2004). Each Landsat TM scene is accompanied by gain and offset values as part of the metadata. The TM band 6 spectral radiance values are subsequently transformed to surface temperature values using the relationship:

$$T_s = \frac{K2}{\ln\left(\frac{K1}{L_\lambda} + 1\right)} \quad (2)$$

where T_s the radiant surface temperature in $K1$ and $K2$ are thermal calibration constants in $Wm^{-2}sr^{-1}$ μm^{-1} supplied by the Landsat Project Science Office (2004), and L_λ is spectral radiance of thermal band pixels in $Wm^{-2}sr^{-1}$ μm^{-1}. For Landsat 7, $K1$ is 666.09 and $K2$ is 12822.71, and for Landsat 5 $K1$ is 607.76 and $K2$ is 1260.56.

The composite emissivity values for urban mosaics are rarely known, but usually assumed to be near 1. The typical emissivity values for man-made surfaces such as concrete and asphalt range from 0.95 to 0.97 (Buettner, 1965). Here, it is important to acknowledge the ambiguity introduced in urban surface temperature distribution by incomplete knowledge of surface emissivity.

Vegetation fraction images were generated from a three-component mixing model based on high albedo substrate, vegetation and dark surface that is physically consistent with the spectral characteristics that might be expected for an urban environment (Small, 2001). Fractional abundance images resulted from a unit sum constrained least squares inversion of the linear mixing model using the spectra of endmembers.

3. RESULTS AND DISCUSSION

The Landsat ETM+ Kuwait City image used in this study was acquired under desert springtime conditions on March 6, 2001, while the New York Landsat ETM+ image was acquired under late summer drought conditions on August 6, 2001. The datasets were subjected to the same processing and enhancement techniques and therefore the dark and light tones in the vegetation fraction and surface temperature images are comparable. The only exception is the Kuwait City vegetation fraction image in which the brightness to contrast ratio has been increased by 30% so that features are observable.

Figure 1 shows Landsat TM bands 7, 4, and 2 color composite images for Kuwait City and New York City. The Kuwait City image clearly shows the demarcation of the residential and the desert areas shown in yellowish-brown. The difference in vegetation density and growth in the various suburbs of Kuwait City is clearly observed in the image. Areas with less vegetation cover, and perhaps needing attention from city planners, include (1) Al-Shuwaikh and Al-Rai, industrial areas with low housing density, (2) Al-Sulaibiyah, (3) Al-Firdous, (4) the scrap metal yard, (5) Doha Village, and (6) Hawalli (Figure 5, Kwarteng and Chavez, 1998). In the New York City image, vegetation in parks, cemeteries, public greenspaces and courtyard are consistently detected. The image clearly distinguishes between residential and industrial areas and highlights the vegetation gradient between the city center and the suburbs. In Manhattan, parks and public greenspace are distinguished and the real differences in street and courtyard vegetation are detected.

Figure 2 shows vegetation fraction and surface temperature images for Kuwait City and New York City derived from Landsat 7 imagery. From Figure 2, the distribution of vegetation fractions observed in Kuwait City is generally lower than that in New York City which has abundant vegetation in the form of large deciduous trees, wetlands and closed canopy forest in parks and cemeteries. In the New York City image, parks and public greenspace are easily distinguished. In addition, interurban differences in street and courtyard vegetation can be consistently detected. Surface temperatures in the suburban areas are in general lower than the residential and industrial areas. Vegetation in Kuwait City consists of palm and shade trees, shrubs, groundcovers, and grass, which are irrigated year round (Kwarteng, 2002a, b). In spite of the low vegetation cover observed in Kuwait City, the relative amounts of the vegetation fractions in different residential areas can be detected in the images. Even though New York City has abundant vegetation, the surface temperatures are higher than Kuwait City, primarily due to the different seasons. The surface temperatures observed for the surrounding desert areas are higher than the built-up areas. Notwithstanding the lower vegetation fractions, the cooling effect is apparent in the clearly defined residential areas in the Kuwait City image (compare Figures 1 and 2).

Each of the scatterplots of surface temperature and vegetation fractions for New York City and Kuwait City show a cloud of a triangular distribution of pixels (Figure 3). Pixels near the base of the triangle, which is parallel to the surface temperature axis, attain a much wider range of temperatures compared to the pixels in the vertex of the triangles. Dark areas in Figure 3 represent higher pixel density than lighter tones.

According to Carlson et al. (1995), the warm edge is a sharply defined boundary representing the locus of highest temperatures and different vegetation fractions. On the other hand, the cold edge represents the locus of lowest temperatures for the vegetation fractions. The triangular shape distribution in the scatterplots define the physical limits imposed by the vegetation cover, soil water content and different combinations of surface materials. In rural areas, the shape of the Temperature/Vegetation (TV) distribution results from spatial variations in vegetation cover and soil moisture availability (Gillies et al., 1997; Crombie et al,, 1999). In urban areas, there is generally little exposed soil so the shape of the distribution is dictated by variations in vegetation cover, albedo and shadow. The TV distributions for New York and Kuwait City do not show the familiar triangular distributions usually seen in rural areas. This is primarily a result of urban land cover heterogeneity and the negligible fraction of exposed moist soil. The warm edge shows a less pronounced cooling effect in New York as the image was acquired during drought conditions with low moisture availability for many areas. The absence of a well-defined cold edge is a consequence of extensive area of the partial shadow at all vegetation fractions. The pervasive presence of shadow in the urban mosaic is a consequence of the characteristic 20-30 m spacing of trees, streets and buildings (Small, 2003) coinciding with the spatial scale of the Landsat

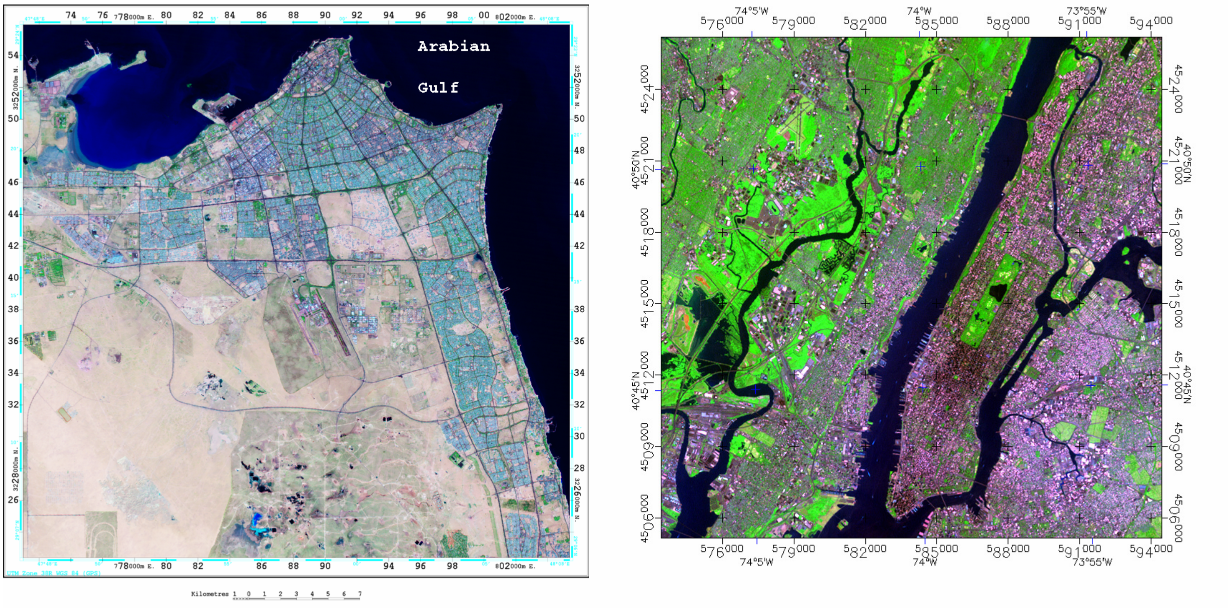

Figure 1. Landsat TM bands 7, 4 and 2 color composite images of Kuwait City (left) and New York City (right) recorded on March 6, 2001 and August 14, 2002, respectively. The near-infrared band, TM band 4, was project through green filters, and therefore, significant vegetation is depicted in shades of green. Built-up areas, with or without vegetation, show up in purple to blue-green colors. Water appears as dark blue to black in both images.

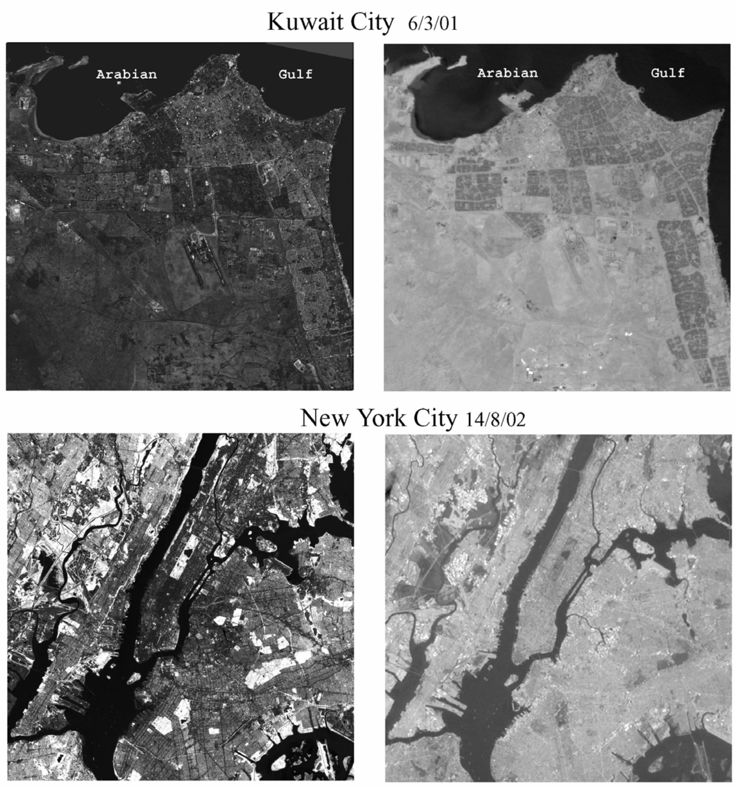

Figure 2. Vegetation fraction and surface temperature images derived from Landsat 7 images for Kuwait City and New York City recorded on March 6, 2001 and August 14, 2002, respectively. Each scene is 30 x 30 km. Grayscale ranges from 0 to 100% for vegetation fractions (left) and from 285 to 315 K (12 to 42°C) for surface temperature (right). Water bodies in the two images, namely the Arabian Gulf and the Upper New York Harbor, the Hudson River and its tributaries have zero vegetation fractions and the minimum temperatures appear in dark tones in the images. The brightness to contrast ratio in the Kuwait City vegetation image has been increased by 30% so that features are visible.

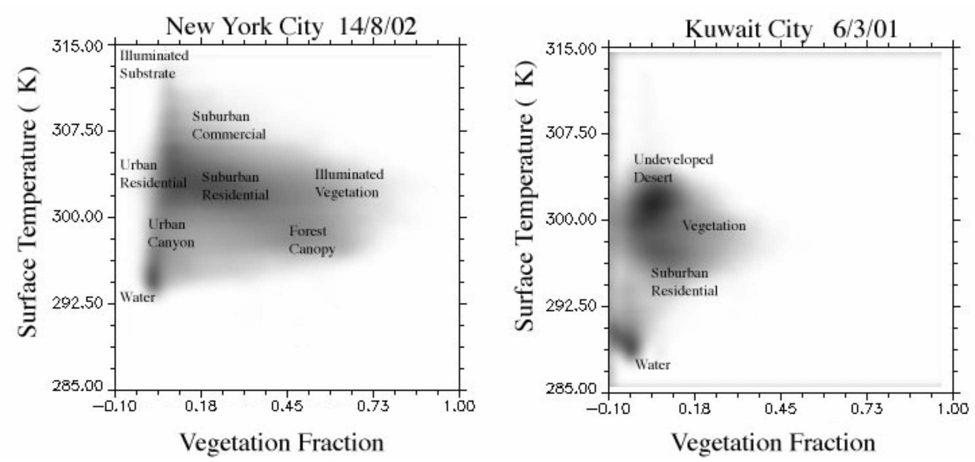

Figure 3. Scatterplots of Surface Temperature and Vegetation Fraction for New York City and Kuwait City. Darker areas correspond to greater number of pixels. Low temperature, unvegetated areas generally correspond to water bodies. Note the Arabian Gulf is cooler in March than in New York Harbor and the surrounding rivers in August. New York also has higher temperatures, in spite of abundant vegetation, because the image was acquired during drought conditions when evapotranspiration was low.

GIFOV. The increase in minimum temperature is more pronounced in the Kuwait City because of the relatively low water temperatures when the image was recorded in the morning of March 6, 2001. Slightly negative vegetation fractions in the Kuwait City image correspond to bare soil that are not accurately represented in the three endmember mixture model. The vegetation fractions in New York City are generally lower than 0.75 as most of the vegetation takes the form of deciduous trees which have as much as 25% internal shadow from canopy structure. In contrast, vegetation fractions in Kuwait City are less that 0.45 because most of the vegetation patches are much smaller than the 30 m GIFOV of the ETM+ sensor.

More land cover categories (Figure 3), identified by locating the geographic position of the pixels in each part of the mixing space, are observed in the New York City than the Kuwait City image primarily due to the morphology and location of the two cities as mentioned previously. Apart from a few tall buildings in the central business district area in the upper-central part along Kuwait Bay, the majority of houses in Kuwait City consists of one or two storey buildings which could be residential, commercial or both. The study area in New York City on the other hand consists of several residential areas with 2 to 20 story buildings and commercial districts containing tall buildings creating urban canyons.

4. CONCLUSIONS

The world's population growth in urban areas will continue to escalate and have a profound effect on environmental conditions and processes. Urban sprawl presents several challenges in the area of land use planning, housing, pollution and development, and changes in microclimate. The most successful applications of remote sensing to the urban environment generally involve measurement of physical quantities related to environmental conditions such as surface temperature and vegetation abundance. Surface temperature distribution and vegetation fraction analysis using Landsat ETM+ data reveal the different energy flux and surface properties for New York City and Kuwait City, located in temperate and desert environments, respectively. Vegetation fraction images are generated from a three-component mixing model based on high albedo substrate, vegetation and dark surface that is physically consistent with the spectral characteristics that might be expected for an urban environment. Surface temperatures are derived from the satellites' thermal infrared band through Planck's law. In Kuwait City the surface temperature of the surrounding desert areas are higher than the residential areas. The cooling effect from vegetation is apparent and is clearly defined in the residential areas. The surface temperatures observed in the residential and commercial areas in the New York City image are higher than the suburban areas. Scatterplots of surface temperature and vegetation fractions define the physical limits imposed by the vegetation cover, soil water content, and different combinations of surface materials in each city.

5. REFERENCES

Akbari, H., 2002. Shade trees reduce building energy use and CO emissions from power plants. *Environmental Pollution*, 116, pp. S119-S126.

Buettner, K.J.K. and C.D. Kern, 1965. The determination of infrared emissivities of terrestrial surfaces. *Journal of Geophysical Research*, 70, pp. 1329-1337.

Carlson, T. N., R.R. Gillies and E. M. Perry, 1994. A method to make use of thermal infrared temperature and NDVI measurements, *Remote Sensing Reviews*, 9, pp. 161-173.

Carlson, T.N., R.R. Gillies and T.J. Schmugge, 1995. An interpretation of methodologies for indirect measurement of soil content water. *Agricultural and Forest Meteorology*, 77, pp. 191-205.

Crombie, M.K., R.R. Gillies, R.E. Arvidson, P. Brookmeyer, G.J. Well, M. Sultan and M. Harb, 1999. An application of remotely derived climatological field for risk assessment of vector-borne disease: A spatial study of filariasis prevalence in the Nile Delta, Egypt. *Photogrammetric Engineering and Remote Sensing*, 65(12), pp. 1401-1409.

Czajkowski, K.P., S.N. Goward, T. Mulhern, S.J. Goetz, A. Walz, D. Shirey, S Stadler, S.D. Prince and R.O. Dubayah, 2004. Estimating environmental variables using thermal remote sensing. In: *Thermal Remote Sensing in Land Surface Processes,* edited by D.A. Quattrochi and J.C. Luvall. CRC Press, Washington D.C., pp. 11-32.

Dash, P., F.-M. Gottsche, F.-S. Olesen and H. Fischer, 2002. Land surface temperature and emissivity estimation from passive sensor data: theory and practice—current trends. *International Journal of Remote Sensing*, 23(13), pp. 2563-2594.

Flynn, L.P., A.J.L. Harris and R. Wright, 2001. Improved identification of volcanic features using Landsat ETM+. *Remote Sensing of Environment*, 78, pp. 180-193.

Gallo, K.P., J.D. Tarpley, A.L. McNab and T.R. Karl, 1995. Assessment of urban heat islands: A satellite perspective. *Atmospheric Research*, 37, pp. 37-43.

Gillies, R. R., T.N. Carlson, J. Cui, W.P. Kustas and K.S. Humes, 1997. Verification of the 'triangle' method for obtaining surface soil water content and energy fluxes from remote measurements of the Normalized Difference Vegetation Index (NDVI) and surface radiant temperature. *International Journal of Remote Sensing*, 18(15), pp. 3145-3166.

Goward, S.N., G.D. Cruickshanks and A.S. Hope, 1985. Observed relation between thermal emission and spectral radiance of a vegetated landscape. *Remote Sensing of Environment*, 18, pp. 137-146.

Howard, L., 1833. *The Climate of London Reduced from Meteorological Observations Made in the Metropolis and Various Places Around It* (2nd Edition) London: A. Arch, Cornhill, Longman & Co.

Kwarteng, A.Y. and P.S. Chavez, Jr., 1998. Change detection study of Kuwait City and environs using multitemporal Landsat Thematic Mapper data. *International Journal of Remote Sensing*, 19(9), pp. 1651-1662.

Kwarteng, A.Y. 2002a. Remote sensing monitoring of greenery development in Kuwait City. In: *Proceedings, 3rd International Symposium on Remote Sensing of Urban Areas*, Istanbul, Turkey, 11-13-June, pp. 337-345.

Kwarteng, A.Y., 2002b. The use of remote sensing imagery to monitor greenery development in Kuwait City. In: *New Technologies for Soil Reclamation and Desert Greenery*, edited by N.M. Al-Awadi and F.K. Taha. Amherst Scientific Publishers, Amherst Massachusetts, pp. 157-177.

Landsat Project Science Office, 2004. Landsat 7 science data user's handbook. Goddard Space Flight Center, NASA, Washington DC. http://ltpwww.gsfc.nasa.gov/IAS/handbook/handbook_toc.html.

Lo, C.P., D.A. Quattrochi and J.C. Luvall, 1997. Application of high-resolution thermal infrared remote sensing and GIS to assess the urban heat island effect. *International Journal of Remote Sensing*, 18, pp. 287-304.

Nichol, J. E., 1996. High-resolution surface temperature patterns related to urban morphology in a tropical city: A satellite-based study. *Journal of Applied Meteorology*, 35, pp. 135–146.

Nichol, J. E., 1998. Visualisation of urban surface temperatures derived from satellite images. *International Journal of Remote Sensing*, 19, pp. 1639-1649.

Nichol, J., 2003. GIS and remote sensing in urban heat island in the Third World. In*: Remotely Sensed Cities*, edited by V. Mesev. Taylor and Francis, New York, pp. 243-264.

Norman, J.M., M. Divakarla and N.S. Goel, 1995. Algorithms for extracting information from remote thermal-IR observations of the Earth's surface. *Remote Sensing of Environment,* 51, pp. 157-168.

Oke, T.R., 1987. *Boundary Layer Climates*. Second edition Methuen: London and New York, pp. 262-302.

Owen, T.W., T.N. Carlson and R.R. Gilles, 1998. An assessment of satellite remotely sensed land cover parameters in quantitatively describing the climatic effect of urbanization. *International Journal of Remote Sensing*, 19, pp. 1663-1681.

Parker, J.H., 1981. *Use of Landscaping for Energy Conservation*. Department of Physical Sciences, Florida International University, Miami, FL.

Price, J. C., 1990. Using spatial context in satellite data to infer regional scale evapotranspiration. *I.E.E.E. Transactions on Geoscience and Remote Sensing*, 28(5), pp. 940-948.

Roth, M., T.R. Oke and W.J. Emery, 1989. Satellite-derived urban heat island from three coastal cities and the utilization of such data in urban climatology. *International Journal of Remote Sensing*, 10, pp. 1699-1720.

Small, C., 2001. Estimation of urban vegetation abundance by spectral mixture analysis. *International Journal of Remote Sensing*, 22(7), pp. 1305–1334.

Small, C., 2003. High spatial resolution spectral mixture analysis of urban reflectance. *Remote Sensing of Environment*, 88, pp. 170-186.

UNPF, 2004. State of world population report 2004. http://www.unfpa.org/swp/swpmain.htm

United Nations, 2001. *The State of the World Cities 2001*. Centre for Human Settlements, UNCHS.

Voogt, J.A. and T.R. Oke, 2003. Thermal remote sensing of urban climates. *Remote Sensing of Environment* 86, pp. 370-384.